Applied Clay Science 62–63 (2012) 1–7

Contents lists available at SciVerse ScienceDirect

Applied Clay Science

journal homepage: www.elsevier.com/locate/clay

Note

An investigation of the catalytic decomposition of formic acid on raw and manganese oxide coated sepiolite surfaces

E. Eren *, H. Gumus, A. Sarihan

Bilecik University, Faculty of Science and Arts, Department of Chemistry, 11210, Bilecik Turkey

ARTICLE INFO

Article history:
Received 15 August 2011
Received in revised form 18 April 2012
Accepted 20 April 2012
Available online 17 May 2012

Keywords:
Sepiolite
γ-MnO_2
Mn_2O_3
Formic acid
Thermal analysis

ABSTRACT

In this study, a mild chemical method was developed to synthesize manganese oxide coated sepiolite from RS, $Mn(NO_3)_2$ and H_2O_2 in an alkaline solution at room temperature. The samples were characterized by X-ray fluorescence (XRF), X-ray diffraction (XRD), infrared (IR) and thermal analysis (TA). After heating up to 600 °C, the structure of the γ-MnO_2 phase gradually transformed into the Mn_2O_3 phase. TA indicated the transformation of γ-MnO_2 into Mn_2O_3 between 400 and 600 °C. IR spectra of manganese oxides showed signature bands between 400 and 650 cm^{-1} due to Mn–O lattice vibrations. The thermal desorption of pyridine was followed by IR and TA techniques to estimate the acidity of the samples. Decomposition of formic acid over RS and MCS was studied by IR spectroscopy at 100–400 °C. Monodentate symmetric and asymmetric formates were observed after formic acid adsorption between 100 and 300 °C.

1. Introduction

Manganese can form a number of oxides due to the different oxidation states. This complex chemistry of manganese oxides provides interesting catalytic properties (Berends et al., 2011; Kovanda and Jirátová, 2011; Yao et al., 2006). Manganese oxides showed high catalytic activity for reactions such as the selective catalytic reduction of NO_x with NH_3 (Tang et al., 2010), the catalytic decomposition of ozone (Gao et al., 2009) and the catalytic combustion of volatile organic compounds (Kim and Shim, 2010).

Carboxylic acids are important elements in the preparation of various commercial products, resulting in appreciable quantities of carboxylic acids in waste streams. Some studies showed that some of these acids, including oxalic, acetic and formic acids, are catalytically oxidized into CO_2 and H_2O at high temperature and pressure (Gomes et al., 2000; Yang et al., 2010). On the other hand, the increase of CO_2 concentration strongly influences the equilibrium condition of weather and environment on earth. For producing clean effluents, it is necessary to characterize the decomposition mechanisms of short-chain acids.

Formic acid is a frequently observed intermediate product of the oxidation of organic wastes in both gas and aqueous phases. Not many studies were conducted to understand the decomposition pathway of short-chain acids in the presence of clay minerals. Raw (RS) and manganese oxide coated sepiolite (MCS) were evaluated in the decomposition proceess of formic acid.

2. Experimental

2.1. Materials

All reagents such as KNO_3, $KMnO_4$, HNO_3, NaOH, and $Mn(NO_3)_2.9H_2O$ were of analytical grade, and all solutions were prepared with twice distilled water.

2.2. Preparation of MCS

20 g of raw sepiolite (RS) were dispersed in 250 mL of 2.0 M NaOH aqueous solution and temperature of the reaction mixture was maintained at 90 °C for 4 h. The base activated RS was dispersed into 150 mL of 0.1 M $Mn(NO_3)_2.9H_2O$ aqueous solution. 300 mL of 0.1 M NaOH aqueous solution was added slowly with a drop rate 1 ml/h. The titration was carried out under nitrogen flow to minimize unexpected reactions e.g. formation of carbonates. The obtained powder was washed with 0.01 M HCl to remove the excess $Mn(OH)_2$ precipitated on the outher surface of the sepiolite and was further washed with deionized water. The oxidation was performed in aqueous dispersions at room temperature. The $Mn(OH)_2$ was dispersed in 50 mL of 1.5 M H_2O_2 at pH 10 and vigorously stirred. The color of the sample immediately turned from original light color to dark brown, indicating the oxidation of the manganese hydroxide into the oxide. To reach equilibrium, the dispersion was further stirred for 24 h. The product was washed with deionized water thoroughly, and the supernatants were filtered off. The solid materials were washed with deionized water repeatedly until the electric conductivity of the filtrate was 1–2 μS/cm (Eren, 2008).

* Corresponding author. Tel.: +90 228 2160101; fax: +90 228 2160287.
E-mail address: erdal.eren@bilecik.edu.tr (E. Eren).

0169-1317/$ – see front matter © 2012 Elsevier B.V. All rights reserved.
doi:10.1016/j.clay.2012.04.013

2.3. Characterization

Infrared (IR) spectra were recorded in the region 4000 to 450 cm^{-1} on a Perkin Elmer Spectrum-100 FTIR (USA) spectrometer. TG and DTA curves were obtained using a Perkin Elmer PRIS Diamond TG/DTG (USA) apparatus in a static air atmosphere (platinum crucibles, mass ~10 mg and temperature range: 30–1000 °C). The XRD analysis data from the samples were collected using a Rigaku, Miniflex ZD13113 (Japan) diffractometer with Cu Kα radiation (Ni fitler). The major elements of the sample were determined by a Spectro X-Lab 2000 (Germany) X-ray fluorescence (XRF) spectrometer. The XRD, XRF and BET analyses were made at the Department of Ceramic Engineering of DumlupinarUniversity.

2.4. Adsorption and decomposition procedures

Batch adsorption experiments were carried out by 0.05 g of adsorbent with 50 ml of formic acid solution of desired concentration (1.2×10^{-2} to 6×10^{-2} M) at room temperature. The equilibrium time was determined as 120 min. After equilibration, the suspensions were centrifuged for 5 min at 3000 rpm and filtered. Supernatants were titrated to determine amount of formic acid with phenolphthalein indicator.

The Brønsted and Lewis acid sites were determined by IR spectroscopy with chemisorbed pyridine. For this purpose, sepiolite samples were dried at 120 °C for 24 h prior to pyridine adsorption. The 50 mg samples were directly contacted with 0.1 mL pyridine. Then, they were kept at 100 °C for 1 h to remove physisorbed pyridine. 3After cooling down to room temperature, the adsorbed pyridine was desorbed for 20 min at several temperatures (100, 200, 300, 400 °C). Specimens for measurement were prepared by mixing 0.9 mg of the sample with 70 mg of KBr and pressing the mixtures into pellets. The IR spectra were recorded between 1400 and 1700 cm^{-1} with 64 scans and at a resolution of 2 cm^{-1}. The reaction between gaseous formic acid and sepiolite was accomplished in desiccators for 2 h at room temperature. Desorption experiments were also done at elevated temperatures (100–400 °C) for 10 min.

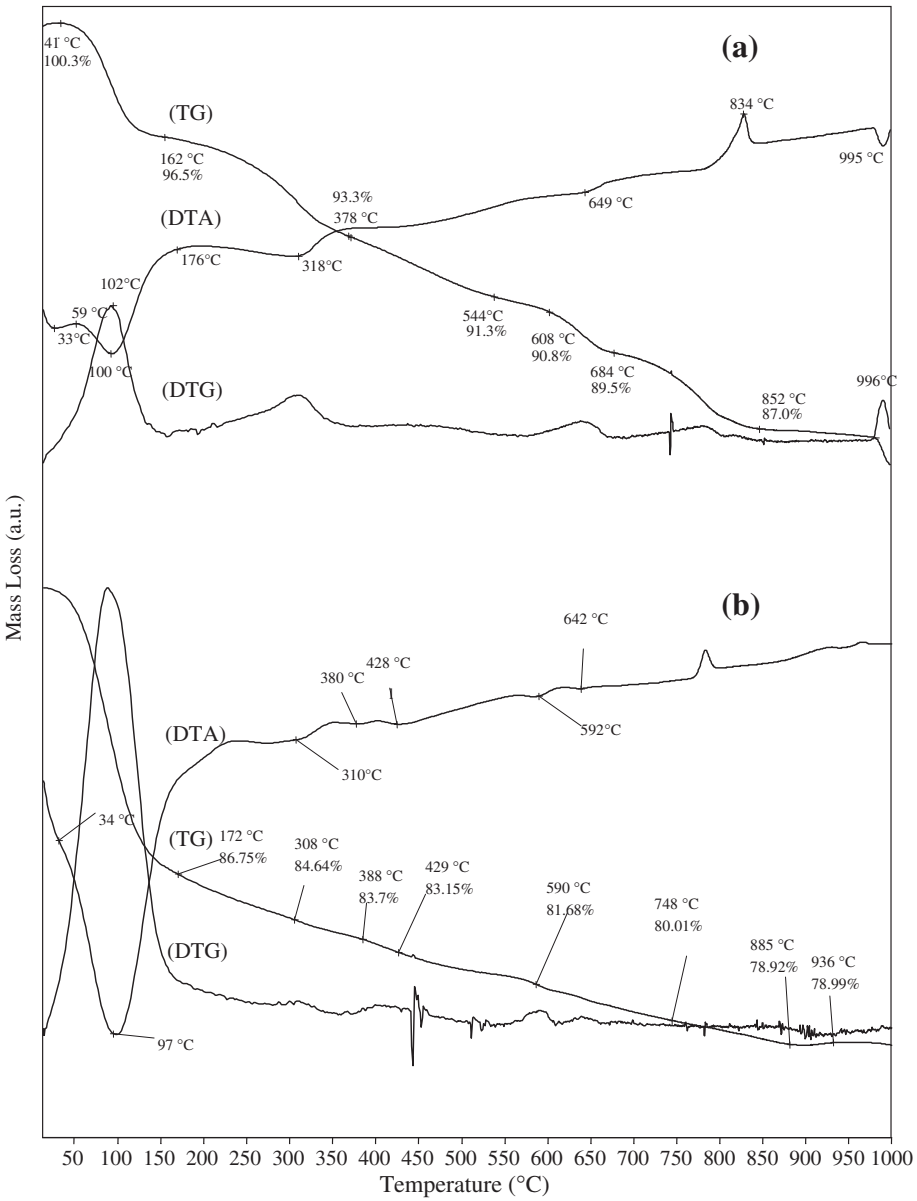

Fig. 1. Thermal analysis curves of (a) RS and (b) MCS samples.

3. Results and discussion

3.1. Material characterization

The chemical composition of RS and MCS are listed in Table S1 (Appendix A; see electronic supplementary material, ESM). The SiO_2 content was taken as a reference because it is a structural element of the sepiolite which is not supposed to change during the manganese oxide coating process. The total content of SiO_2 and MgO of RS was 85.05% and the ratio SiO_2/MgO was 1.81. The total content of SiO_2 and MgO of MCS was 41.48% and SiO_2/MgO was 2.88. This result indicated the extraction of Mg^{2+} cations from sepiolite during the manganese oxide coating process.

The XRD patterns of RS and MCS samples are shown in Fig. S2. The basal reflection of sepiolite was intense and appeared at $2\theta = 7.7°$. The 36.5° reflection of γ-MnO_2 is somewhat higher than the (110) reflection of sepiolite. The XRD pattern of manganese oxide exhibited the well-defined 120, 131, 230, 160, 242 reflections of γ-MnO_2 planes, respectively (Fig. S1b). In the XRD pattern of MCS the reflections of sepiolite were smaller than that of γ-MnO_2. The profiles of the γ-MnO_2 reflections at $2\theta = 19.2°$, 37.1°, 39.4°, 56.3°, 67.5° were broadened. A reflection at $2\theta = 66.8°$ indicated the presence of δ-MnO_2 phase. The broadening of the reflections and their reduced intensity may be attributed to the dispersion of the γ-MnO_2 particles on the surfaces of the sepiolite. According to the XRD patterns (Fig. S1c), the γ-MnO_2 structure remained unchanged after heating at 200 °C for 20 min, indicating that the desorption of the crystal water did not damage the γ-MnO_2 structure. After heating at 400 °C, the XRD pattern of MCS showed the 332, 431, 440, and 444 reflections of Mn_2O_3 (Zhu and Hill, 2002). The broadening of the reflections indicated that the particles were small and/or of low crystallinity.

The TG data of RS exhibited mass losses of 6.8% at 30–376 °C and 6.5% at 376–987 °C due to the desorption of adsorbed water, and dehydroxylation (Karamanis et al., 2011). MCS revealed mass losses of 14.9 and 6.2% at 30–376 °C and 376–972 °C. The mass loss of MCS at 30 to 200 °C was higher than that of RS. MCS had endothermic peaks at 97, 310, 428 and 592 °C (Fig. 1b). The endothermic peak at 97 °C was assigned to the evaporation of adsorbed water. The loss of 1.9% at 200–350 °C was attributed to dissociatively chemisorbed water, strongly bound micropore water and hydroxyl groups in the interior of the lattice (Malankar et al., 2010). These data indicated the partial transformation of MnO_2 to Mn_2O_3, which was identified by XRD after heating at 600 °C. The endothermic peak at 592 °C indicated that the phase transition from γ-MnO_2 to Mn_2O_3 at 428 °C was not complete and that γ-MnO_2 was very slowly converted into Mn_2O_3. The exothermic peaks observed at 834 and 810 °C for RS and MCS were assigned to the phase transformation of sepiolite to enstatite ($MgSiO_3$). The lower enstatite formation temperature of MCS indicated the alteration in the proportion and the position of the Mg cation within the octahedral sheet (Kulbicki, 1959).

The IR spectrum of MCS showed that the band at 1206 cm^{-1} did not change after manganese oxide coating (Fig. 2) as it originates from the Si—O—Si bonds between the ribbons of palygorskite and sepiolite (Frost et al., 2010). Noticeable changes in band positions were detected between 900 and 400 cm^{-1} for MCS. The small shift of the 532 cm^{-1} band to 524 cm^{-1} indicated the involvement of Si—O bonds in the coating process (Sarı et al., 2007, 2010). The absorption bands at 645 and 689 cm^{-1} for RS were due to the Mg_3OH bending (Chahi et al., 2002; Suárez and García-Romero, 2006). After coating process, the Mg_3OH bending bands turned into a broadened and asymmetrical band and shifted to 638 cm^{-1} (Fig. 2). This revealed structural changes of the octahedral sheets were accompanied by changes in the composition as revealed by XRF. Some changes of their position and intensity showed the structural changes of MCS by heating. The vibrational mode corresponding to the bands centered

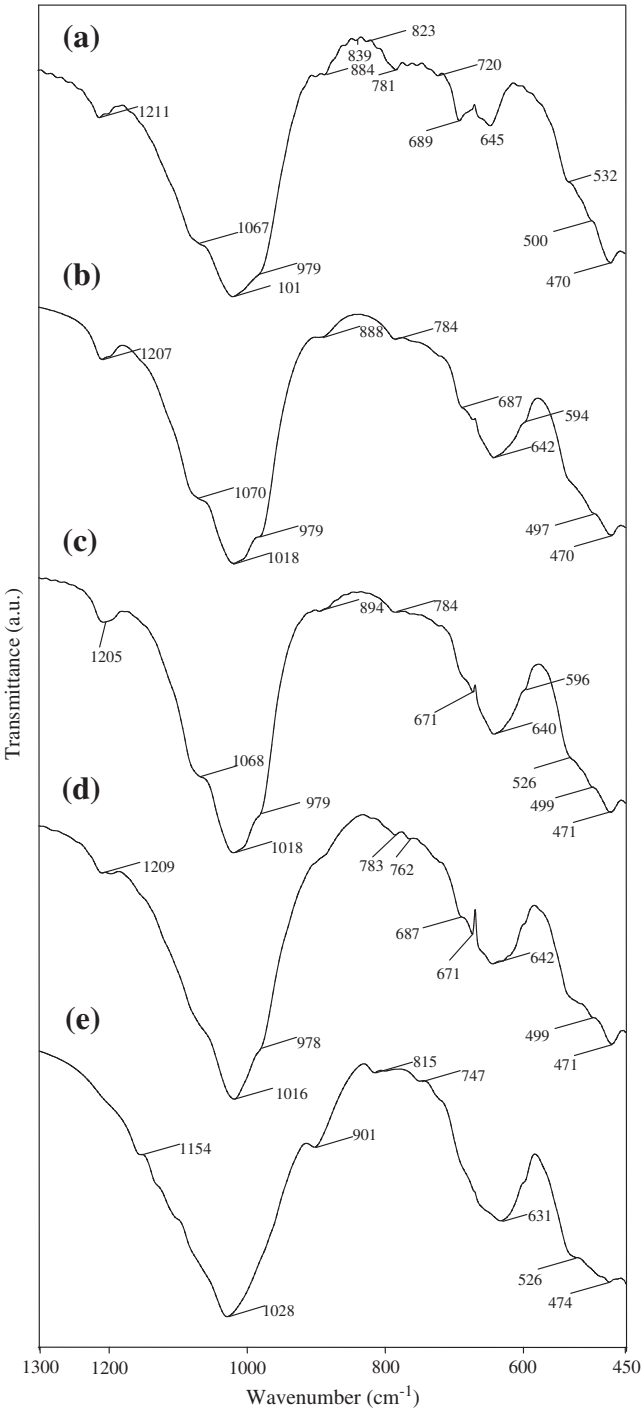

Fig. 2. IR spectra of (a) RS; (b) γ-MnO_2; (c) MCS heated in air at 200 °C for 20 min; (d) MCS heated in air at 400 °C for 20 min; (e) MCS heated in air at 600 °C for 20 min.

at 671 and 642 cm^{-1} is characteristic of MnO_2 structure (Wu et al., 2010; Zhang et al., 2007). When the temperature was increased to 600 °C, the band at 671 cm^{-1} almost disappeared, confirming the transformation of the MnO_2 into Mn_2O_3, in agreement with the XRD and TA data.

3.2. Surface acidity of the sepiolite samples

The IR spectra between 1400 and 1700 cm^{-1} after thermal desorption of adsorbed pyridine are presented in Fig. 3. The bands at

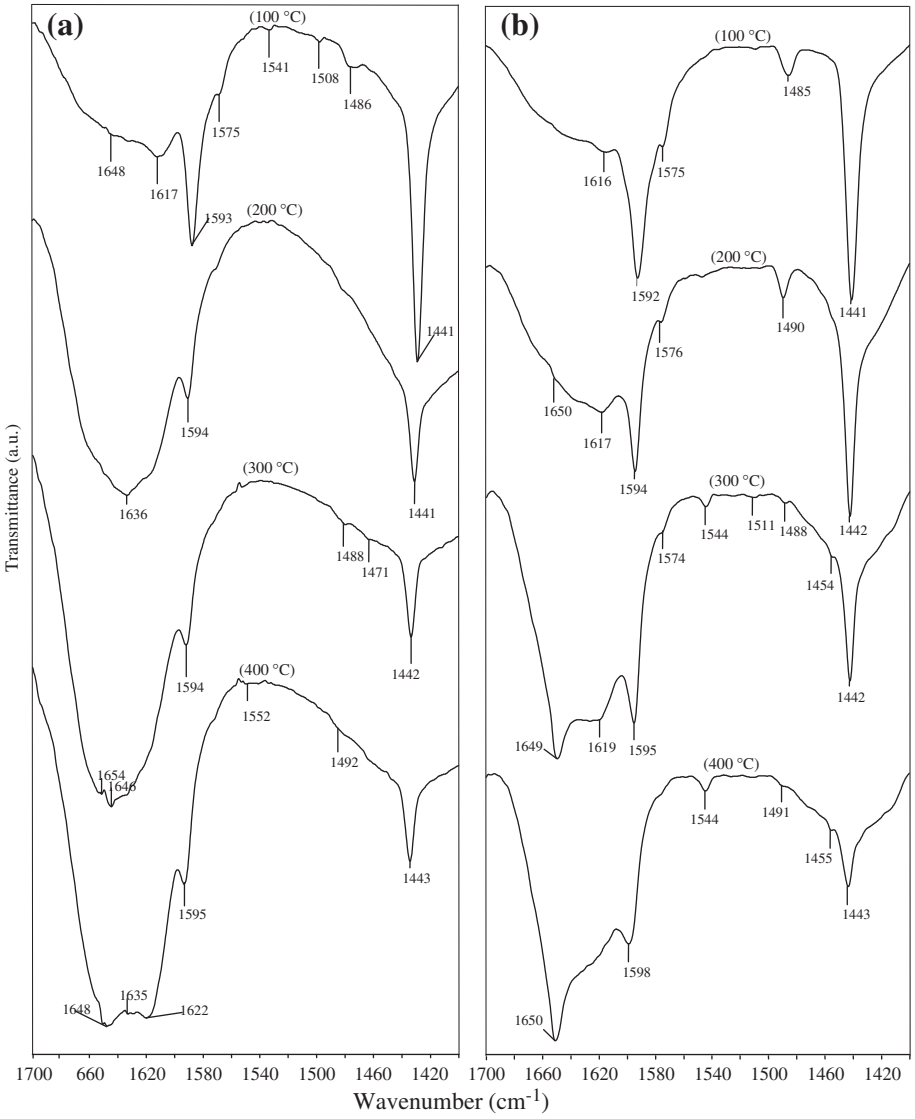

Fig. 3. Desorption of pyridine from sepiolite samples between 100 and 400 °C: (a) RS, (b) MCS.

1443 and 1595 cm^{-1} for RS/Py were stable during the desorption at 400 °C and, therefore, were not assigned to hydrogen-bond pyridine, which is desorbed at temperature as low as 100 °C (Shimizu et al., 2008; Zaki et al., 2001). After heating at 200 and 400 °C, a very broad band was observed around 1640 cm^{-1} corresponding to water and pyridine bound at Lewis sites of RS/Py. Pyridine adsorbed on Lewis sites was still observed at 400 °C as indicated by the bands at 1622, 1595 and 1443 cm^{-1}. The band around 1622 cm^{-1} may be attributed to the another type of Lewis sites (Risemana et al., 1985; Scokart et al., 1979). Thus, the acid sites of RS were predominantly of Lewis acid character. Similar bands were observed in the case of MCS/Py (Fig. 3). The band at 1441 cm^{-1} indicating Lewis acid sites shifted to 1443 cm^{-1} after desorption at 400 °C. After heating at 300 °C, the bands observed at 1595 and 1619 cm^{-1} indicated two types of pyridine which were directly coordinated to the metal cations. At the same temperature, the band at 1544 cm^{-1} was due to Brønsted acid bound pyridine. Furthermore, pyridine adsorbed on Brønsted sites was still stable at 400 °C as indicated by the band at 1544 cm^{-1}. This result indicates that hydroxyl groups of MCS have an acid high enough to protonate the pyridine.

The amount of desorbed pyridine can be considered as the amount of the acid sites on the sample. The total mass loss up to 1000 °C as 32.7 for RS/Py and 19.9% for MCS/Py (Fig. 4). Thus, RS showed a higher amount that the amount of acid sites than MCS. However, for RS/Py sample, the major amount of pyridine desorption occured in the weak acid strength (30–250 °C) region (Campelo et al., 2002; Thomas and Sugunan, 2006). The amount of pyridine desorbed up to 250 °C was 66% for RS/Py and and ≈46% for MCS/Py. The amount of pyridine desorbed between 250 and 400 °C was 10% for RS/Py and ≈22% for MCS/Py. The desorption of adsorbed pyridine at 250–400 °C indicated pyridine mainly bound on Brønsted acid sites. Thus, this result also indicated an increased Brønsted acidity after manganese oxide coating.

3.3. Adsorption and desorption of formic acid from the sepiolite samples

Langmuir monolayer adsorption capacity of the MCS (96.13 mg/g) was found greater than that of the RS (63.08 mg/g). The IR spectra measured for formic acid adsorbed RS (RS/FA) and MCS (MCS/FA) at different temperatures are shown in Fig. 5. After heating to higher temperatures, some changes were observed in the shape of the peaks located between 1200 and 4000 cm^{-1}. The formation of formates was investigated by analyzing the C—H stretching vibrations (set of bands at around 2900 cm^{-1}). As shown in Fig. 5, the related C—H stretching vibration at 2881 cm^{-1} confirmed the presence of formate species (Araujo et al., 2008; Pigos et al., 2007). After heating

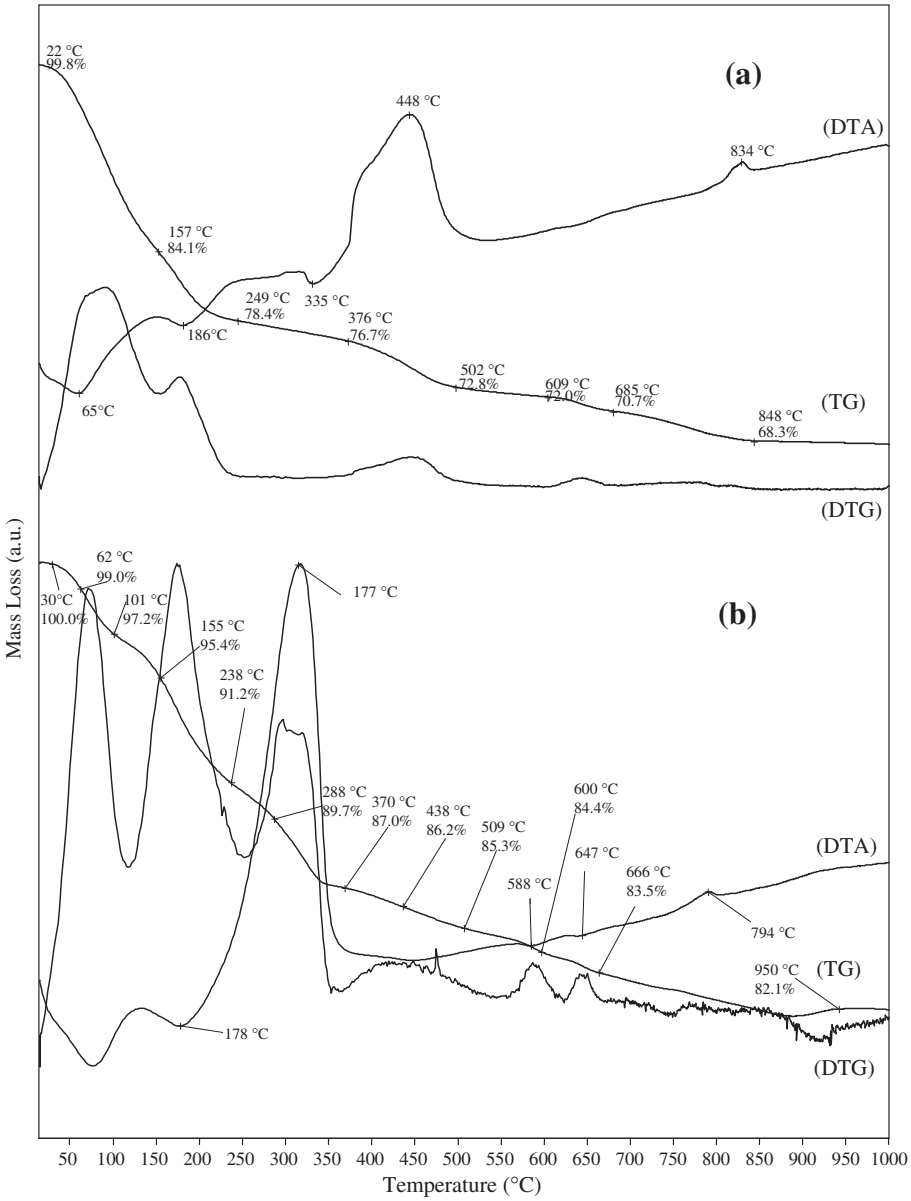

Fig. 4. Thermal analysis curves of the (a) RS/Py and (b) MCS/Py samples.

at 300 °C, the intensity of the C—H stretching vibration was reduced and disappeared above 400 °C. The band at 2162 cm^{-1} for MCS/FA sample was attributed to the carbon monoxide from the decomposition of formic acid. The peaks at 1566–1581 and 1337–1356 cm^{-1} corresponded to formate OCO the asymmetric and symmetric stretching vibration of formate OCO (Miller et al., 2010). After heating from 100 to 200 °C, the OCO asymmetric band shifted from 1566 to 1581 cm^{-1}, the OCO symmetric band at 1356 broadened, and the C—H formate band at 2881 cm^{-1} shifted to 2901 cm^{-1}. The decreasing intensity of the bands at 1364 and 1588 cm^{-1} showed that the amount of formate species had a maximum value at 100 °C and then decreased strongly at 300 °C (Cazata and Primet, 1986; Edwards and Schrader, 1985; Fonseca et al., 2004).

The arrangement of formate ions on the surface was derived by examining the frequency difference between the asymmetric and symmetric OCO stretching vibration bands, denoted as $\Delta\nu_{as\text{-}s}$, relative to aqueous ionic formate ($\Delta\nu_{ionic} = 201\ cm^{-1}$) (Dolamic and Burgi, 2006; Miller et al., 2010). Miller et al. (2010) described the correlations between $\Delta\nu_{as\text{-}s}$ and the arrangement of formate ions as $\Delta\nu_{as\text{-}s} > \Delta\nu_{ionic}$ = monodentate coordination; $\Delta\nu_{as\text{-}s} < \Delta\nu_{ionic}$ = chelating or bidentate bridging; $\Delta\nu_{as\text{-}s} << \Delta\nu_{ionic}$ = bidentate chelating. After heating from 100 to 200 °C, the asymmetric OCO band shifted from 1566 to 1592 cm^{-1}, and the symmetric one from 1356 to 1337 cm^{-1}. The $\Delta\nu_{as\text{-}s}$ value increased from 210 to 255 cm^{-1} with incrasing temperature. Thus, formate was adsorbed in monodentate configuration on the MCS surface.

4. Conclusion

An efficient and sustainable technology has to be developed for the separation of carboxylic acids from the waste water stream from the points of view of pollution control and recovery of useful materials. Formic acid is a fundamental compound in the effluent of chemical industries. The present study focused on developing a catalyst for the decomposition of formic acid. Sepiolite, a clay mineral with high adsorption capacity and manganese oxide as catalyst were selected. MCS were prepared using a mild preparation route. The adsorption of formic acid on MCS sample was approximately 1.5 times higher than that for raw sepiolite. Due to the high formic acid adsorption

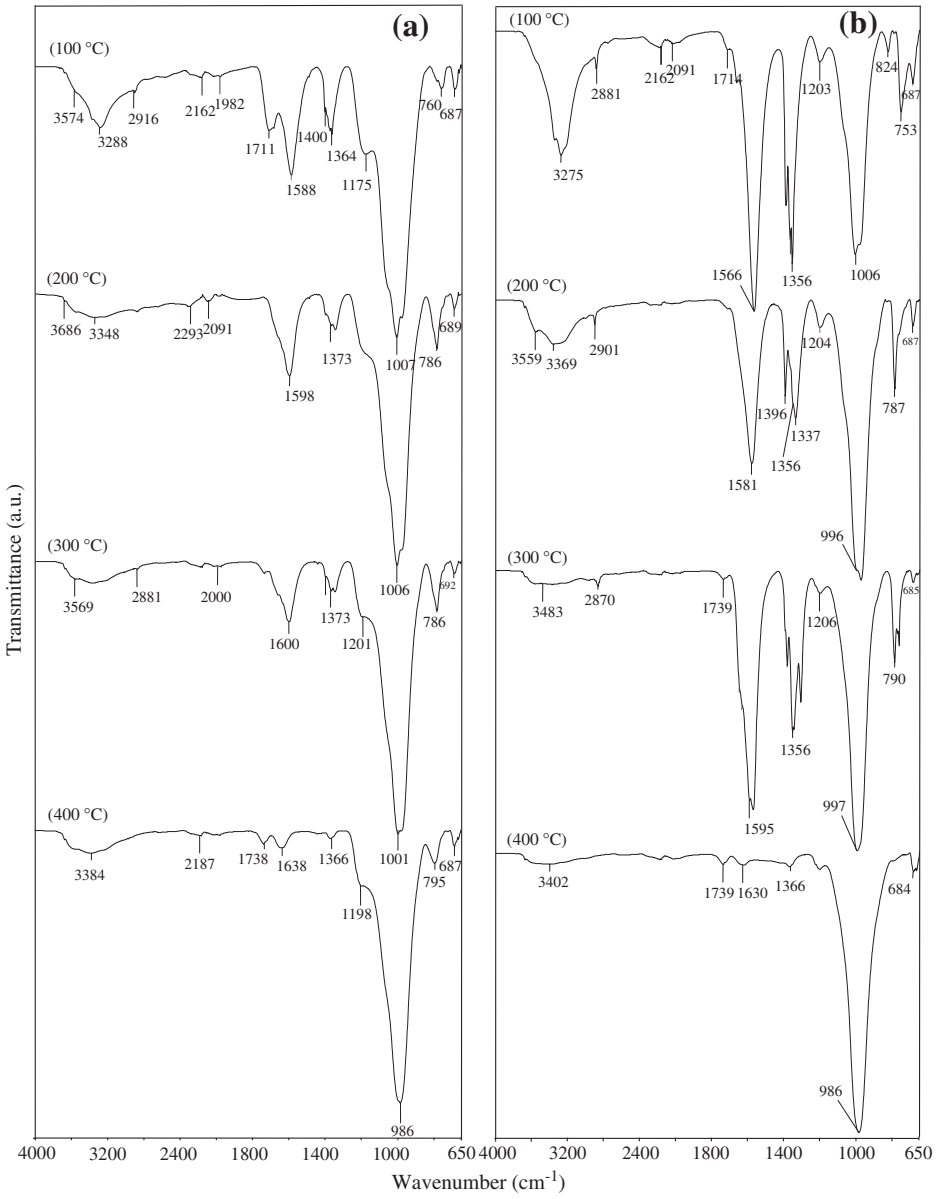

Fig. 5. IR spectra of formic acid species adsorbed on sepilite samples between 100 and 400 °C: (a) RS, (b) MCS.

of MCS and its thermal decomposition, maganese oxide coated sepiolite has a high potential for environmental applications.

Acknowledgments

The authors would like to thank Prof. Dr. Gerhard Lagaly (University of Kiel, Germany) and Reviewers for their remarks and corrections of the manuscript.

Appendix A. Supplementary data

Supplementary data to this article can be found online at http://dx.doi.org/10.1016/j.clay.2012.04.013.

References

Araujo, J.C.S., Zanchet, D., Rinaldic, R., Schuchardt, U., Horid, C.E., Fierroe, J.L.G., Bueno, J.M.C., 2008. The effects of La_2O_3 on the structural properties of La_2O_3–Al_2O_3 prepared by the sol–gel method and on the catalytic performance of Pt/La_2O_3–Al_2O_3 towards steam reforming and partial oxidation of methane. Applied Catalysis B: Environmental 84, 552–562.

Berends, H.-M., Homburg, T., Kunz, I., Kurz, P., 2011. K10 montmorillonite supported manganese catalysts for the oxidation of water to dioxygen. Applied Clay Science 53, 174–180.

Campelo, J.M., Leon, R.M., Luna, D., Marinas, J.M., Romero, A.A., 2002. Catalytic activity, deactivation and re-use of Al–MCM-41 for N-methylation of aniline. Studies in Surface Science and Catalysis 142, 1299–1306.

Cazata, J.T., Primet, M., 1986. Surface species involved during the hydrogenation of CO on a Rh/ThO_2 catalyst. Applied Catalysis 24, 163–174.

Chahi, A., Petit, S., Decarreau, A., 2002. Infrared evidence of dioctahedral–trioctahedral site occupancy in palygorskite. Clays and Clay Minerals 50, 306–313.

Dolamic, I., Burgi, T., 2006. Photoassisted decomposition of malonic acid on tio_2 studied by in situ attenuated total reflection ınfrared spectroscopy. The Journal of Physical Chemistry. B 110, 14898–14904.

Edwards, J.F., Schrader, G.L., 1985. Methanol, formaldehyde, and formic acid adsorption on methanol synthesis catalysts. Journal of Physical Chemistry 89, 782–788.

Eren, E., 2008. Removal of copper ions by modified Unye clay, Turkey. Journal of Hazardous Materials 159, 235–244.

Fonseca, A.A., Gardnera, P., Torbati, R., Sakakini, B.H., Waugh, K.C., 2004. The determination of desorption rate constants by monitoring of the time dependence of the decay of infrared bands-dynamic infrared spectroscopy. Journal of Catalysis 221, 313–318.

Frost, R.L., Xi, Y., He, H., 2010. Synthesis, characterization of palygorskite supported zero-valent iron and its application for methylene blue adsorption. Journal of Colloid and Interface Science 341, 153–161.

Gao, L., Zhai, Y., Ma, H., Wang, B., 2009. Degradation of cationic dye methylene blue by ozonation assisted with kaolin. Applied Clay Science 46, 226–229.

Gomes, H.T., Figueiredo, J.L., Faria, J.L., 2000. Catalytic wet air oxidation of low molecular weight carboxylic acids using a carbon supported platinum catalyst. Applied Catalysis B: Environmental 27, L217–L223.
Karamanis, D., Ökte, A.N., Vardoulakis, E., Vaimakis, T., 2011. Water vapor adsorption and photocatalytic pollutant degradation with TiO_2–sepiolite nanocomposites. Applied Clay Science 53, 181–187.
Kim, S.C., Shim, W.G., 2010. Catalytic combustion of VOCs over a series of manganese oxide catalysts. Applied Catalysis B: Environmental 98, 180–185.
Kovanda, F., Jirátová, K., 2011. Supported layered double hydroxide-related mixed oxides and their application in the total oxidation of volatile organic compounds. Applied Clay Science 53, 305–316.
Kulbicki, G., 1959. High temperature phases in sepiolite, attapulgite and saponite. American Mineralogist 44, 752–764.
Malankar, H., Umare, S.S., Singh, K., Sharma, M., 2010. Chemical composition and discharge characteristics of γ-MnO_2 prepared using manganese ore. Journal of Solid State Electrochemistry 14, 71–82.
Miller, K.L., Lee, C.W., Falconer, J.L., Medlin, J.W., 2010. Effect of water on formic acid photocatalytic decomposition on TiO_2 and Pt/TiO_2. Journal of Catalysis 275, 294–299.
Pigos, J.M., Brooks, C.J., Jacobs, G., Davis, B.H., 2007. Low temperature water–gas shift: the effect of alkali doping on the CH bond of formate over Pt/ZrO_2 catalysts. Applied Catalysis A: General 328, 14–26.
Risemana, S.M., Bandyopadhyaya, S., Massotha, F.E., Eyring, E.M., 1985. Photoacoustic spectroscopy of pyridine chemisorbed on calcined and sulfided molybdenum catalysts. Applied Catalysis 16, 29–37.
Sarı, A., Tuzen, M., Soylak, M., 2007. Adsorption of Pb(II) and Cr(III) from aqueous solution on Celtek clay. Journal of Hazardous Materials 144, 41–46.
Sarı, A., Çıtak, D., Tuzen, M., 2010. Equilibrium, thermodynamic and kinetic studies on adsorption of Sb(III) from aqueous solution using low-cost natural diatomite. Chemical Engineering Journal 162, 521–527.
Scokart, P.O., Selim, S.A., Damon, J.P., Rouxhet, P.G., 1979. The chemistry and surface chemistry of fluorinated alumina. Journal of Colloid and Interface Science 70, 209–222.
Shimizu, K., Higuchi, T., Takasugi, E., Hatamachi, T., Kodama, T., Satsuma, A., 2008. Characterization of Lewis acidity of cation-exchanged montmorillonite K-10 clay as effective heterogeneous catalyst for acetylation of alcohol. Journal of Molecular Catalysis A: Chemical 284, 89–96.
Suárez, M., García-Romero, E., 2006. FTIR spectroscopic study of palygorskite: influence of the composition of the octahedral sheet. Applied Clay Science 31, 154–163.
Tang, X., Li, J., Sun, L., Hao, J., 2010. Origination of N_2O from NO reduction by NH_3 over β-MnO_2 and α-Mn_2O_3. Applied Catalysis B: Environmental 99, 156–162.
Thomas, B., Sugunan, S., 2006. Rare-earth (Ce^{3+}, La^{3+}, Sm^{3+}, and Re^{3+}) exchanged Na-Y zeolites and K-10 clay as solid acid catalysts for the synthesis of benzoxazole via Beckmann rearrangement of salicylaldoxime. Microporous and Mesoporous Materials 96, 55–64.
Wu, F., Li, J., Qin, Q., Li, Z., Huang, X., 2010. Facile synthesis of γ-MnOOH micro/nanorods and their conversion to β-MnO_2. Mn_3O_4. Journal of Alloys and Compounds 492, 339–346.
Yang, S., Besson, M., Descorme, C., 2010. Catalytic wet air oxidation of formic acid over $Pt/Ce_xZr1-xO_2$ catalysts at low temperature and atmospheric pressure. Applied Catalysis B: Environmental 100, 282–288.
Yao, S., Yuan, S., Xu, J., Wang, Y., Luo, J., Hu, S., 2006. A hydrogen peroxide sensor based on colloidal MnO_2/Na-montmorillonite. Applied Clay Science 33, 35–42.
Zaki, M.I., Hasan, M.A., Al-Sagheer, F.A., Pasupulety, L., 2001. In situ FTIR spectra of pyridine adsorbed on SiO_2–Al_2O_3, TiO_2, ZrO_2 and CeO_2: general considerations for the identification of acid sites on surfaces of finely divided metal oxides. Colloids and Surfaces A: Physicochemical and Engineering Aspects 190, 261–274.
Zhang, L., Liu, Z.-H., Tang, X., Wang, J., Ooi, K., 2007. Synthesis and characterization of β-MnO_2 single crystals with novel tetragonous morphology. Materials Research Bulletin 42, 1432–1439.
Zhu, H.J., Hill, R.H., 2002. The photochemical metal organic deposition of manganese oxide films from films of manganese(II) 2-ethylhexanoate: a mechanistic study. Journal of Non-Crystalline Solids 311, 174–184.